Aggregation modeling of large wind farms using an improved *K*-means algorithm

Jian-ping Zhang, Hao-zhong Cheng, Shu-xin Tian and Ding Yan
Key Laboratory of Control of Power Transmission and Conversion, Ministry of Education
Department of Electrical Engineering
Shanghai Jiao Tong University
800 Dongchuan Rd., Shanghai 200240 China
Email zjp42132@139.com; hzcheng@sjtu.edu.cn; tsx396@163.com; 15821801855@163.com

Abstract: - Large wind farms require modeling and simulation in their planning and construction process to provide a basis for grid planning. As a large wind farm is comprised of hundreds or even thousands of wind generators, the detailed-model building of wind farms is difficult, which are associated with slow simulation speeds and heavy workloads. In this paper, an improved *K*-means algorithm-based aggregation modeling method is proposed for large wind farms. A model is built for a typical 300 MW wind farm of the northern Jiangsu Province in China and its simulations are performed. The results based on a comparison between a single-fan aggregation model and a multi-fan aggregation model are obtained. The aggregation method proposed in this paper proves to be accurate and fast, which is able to meet the requirements for output simulation.

Key-words: - wind farm, power grid, wind generator, aggregation modeling, output simulation, *K*-means clustering algorithm.

1 Introduction

With the development of wind-power technology, large wind farms are continuously being connected into the power grid. The volatility of these plants affects the quality, reliability, and stability of the power grid [1,2]. To study the operational characteristics of a wind farm, it is necessary to plan and construct the grid structure, as well as accurately built equivalent model and predict the output of the wind farm before large-scale wind power penetration.

The wake effect of a fan directly influences the output of a wind farm [3]. At the same time, due to the differences in the locations of the distributed fans and randomness in the wind speed, the disparate wind speeds incident on each fan increases the complexity of the modeling. In addition, the planning and application of a real power grid calls for simple models and fast simulation speeds. Therefore, an effective aggregation modeling method is needed to complete the work introduced above [4-6]. In similar work [7-9], single-fan equivalent models are built based on the operation data of detailed –model for wind farm. Owing to large distributional regions of wind farm and the impacts of wake effect and geomorphic feature, the single–fan model is only applied to some studies with low simulation accuracy. So an equivalent modeling method with the high simulation accuracy and parameters optimization model of a wind farm are proposed by using the operational data of a DFIG wind farm with the detailed models Regarding DFIGs with different parameters the dynamic and transient performances are simulated and analyzed The results are also compared with those by using the detailed model and the capacity weighted equivalent model of the DFIG wind farm The results show that the proposed wind farm equivalent model has the same wind farm operation characteristics with the detailed model and it has better representation of the

dynamic and transient performances of the wind farms.

2 Fan aggregation modeling using single-fan characterization

Single-fan characterization method is one of the commonest methods of aggregation modeling used for the fans in wind farms at present. In this method, the wind farm is deemed to be equivalent to a wind turbine and an generator. The main features of the aggregation method are as indicated below [10]:

(1)Determine the rated capacity of the wind turbine.

(2)Determine the corresponding capacity increment of booster transformer.

(3)Determine the short-circuit capacity of the infinite system.

(4)Determine the value of the overcurrent protection setting of the rotor.

(5)Determine the shafting parameter of the fan set.

(6)Determine the reference value of the power measurement module in the power frequency conversion control system of the rotor.

(7)Determine the average air density on the premise of a constant blowing area of the wind wheel.

The single-fan equivalence method is suitable for aggregation modeling of small wind farms due to its simple and efficient calculation process. However, its accuracy is not satisfactory when applied to large wind farms considering the influence of geographical conditions and the wake effect of the fans.

3 Fan aggregation modeling using multi-fan characterization

3.1 Basic principles

In order to accurately characterize the output properties of a large wind farm, simplify the aggregation model, and shorten the model's simulation time, this paper proposes a multi-fan characterized aggregation model for wind farm. In this model, the fans in the large wind farm are classified according to their operation characteristics. The fans on adjacent operation points are classified as a single class. Moreover, fans of the same class are aggregated into one fan.

3.2 Classification indices for fans

To reasonably and objectively classify the large number of fans in the wind farm, a classification index is required to accurately reflect the operation point of the fans [11-15].

This study investigates the output of the wind farm in the steady state. Due to the differences of the input wind speeds, the fans in the wind farm are placed in different locations. As the wind speed set in the simulation is the mean wind speed, there is no need to take into account the storage and release of the fan rotator energy induced by wind speed fluctuation. Therefore, wind speed can be used as the classification index for the fans.

3.3 Fan classification using the K-means clustering algorithm

In statistics, the K-means algorithm is one of widely used clustering algorithms. The key feature of the algorithm is that N sample points are classified into K clusters based on the principle of minimizing a standard measurement function. Sample points in the same cluster have a high degree of similarity, while those in different clusters show lower degrees of similarity. Different methods of selecting the initial center value used for clustering lead to the K-means algorithm showing disparate clustering accuracy and convergence degrees [16-24]. Generally the K-means algorithm is carried out according to the following steps:

(1) Randomly select K sample points to act as

the initial cluster centers.

(2) Allocate the residual N – K sample points to their nearest clusters according to the distance between the sample point and each cluster center.

(3) Calculate the sample mean of each cluster m and the value expressions of the standard measurement function E are given by

$$m_i = \frac{1}{N_i}\sum_{\tau \in Ci} \tau \, , E = \sum_{i=1}^{K}\sum_{\tau \in Ci} \left|\tau - m_i\right|^2 \qquad (1)$$

where m_i is the mean of sample cluster i, τ is a sample point, C_i is the set of sample points in cluster i, and N_i is the number of sample points in cluster i.

(4) Substitute the initial cluster center with the sample means from each cluster and repeat steps (2)–(4) until the standard measurement function converges.

It can be seen from the steps above that the algorithm is heuristic, i.e. the convergence of the K-means algorithm is greatly affected by the initial values selected. Therefore, there is no guarantee that the final convergence results represent the optimum solution desired. This problem is solved by repeating the calculation multiple times. The initial values in each set of calculations are randomly selected and are different each time. Finally, the results obtained from each set of calculations are compared to determine the solution with the minimum measurement function. This is taken to be the optimum solution desired.

In this study, the wind speed including the wind wake effect is used for the clustering index of the fan. As the fans are distributed according to a certain law, when initial wind speed is constant, the wind speeds among the fans are similar to each other and show a decreasing order. Therefore, the initial clustering centers selected for the K-means algorithm are K-2 points between the maximum and minimum wind speeds, as well as the minimum and maximum wind speeds themselves.

In the standard K-means algorithm, K is given a constant value. In this study, K is merely given the initial value K_0 and an upper limiting value of K_{max}, and K is allowed to increase from K_0 to K_{max}. Generally, the larger the value of K, the smaller the value of measurement function, and the more accurate the model. As the value of K increases, the value of measurement function is smaller than a certain given value, the circulation is terminated. The value of K here is the final value. Under the special condition that $n_0<K_{max}$, where n_0 is the number of kinds of wind speed, the measurement function is zero when $K=n_0$ and fan clustering has achieved the optimum state.

3.4 Aggregation modeling

After the clustering calculation on the fans has finished according to the steps above, the fans in the same cluster can be parameterized and aggregated using the single-fan equivalent method. As the fans in the same cluster are highly similar, the aggregated model is more accurate [25]. After aggregation, the input wind speed of each equivalent fan is set to the mean wind speed of corresponding fan cluster.

4 Fan aggregation modeling of a typical wind farm in northern Jiangsu

4.1 Detail model of wind farm

A 300 MW wind farm in northern Jiangsu Province was chosen for analysis. Fig.1 shows the fan layout in this wind farm. The fans used in this plant are SL3000/113 doubly-fed induction generators (DFIGs) [26]. Each fan has a unit capacity of 3 MW, impeller diameter of 113 m, hub height of 90 m, cut-in wind speed of 3 m/s, cut-out wind speed of 25 m/s, and a rated wind speed of 11.6 m/s [27].

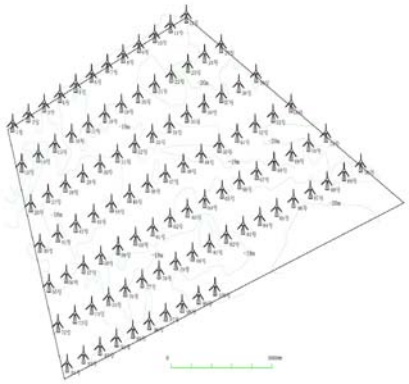

Fig.1. The wind farm in northern Jiangsu

The direction that is vertical to the first row of fans from the inside out is taken to be the positive direction. To compare the output under different wind speeds, four typical simulation scenarios are introduced in this study: (1) 11.6 m/s in the positive direction at an angle of incidence of 0° (i.e. the rated conditions); (2) 15 m/s in the positive direction at 30°; (3) 9 m/s in the positive direction at 60°; (4) 11.6 m/s in the positive direction at 90° (the worst case scenario). Appendix Table 1 lists the equivalent input wind speeds of each fan under the different conditions.

A simplified DFIG model was used for the single-fan model. Then, by adjusting the parameters in this simplified model, a single-fan simplified model of a 3 MW fan in this plant was obtained. Finally, a detailed model of the wind farm (100 fans) was established.

Fans with exactly the same input speed were simplified as multiple identical fans in parallel and expressed as one fan multiplied by the number of fans based on DIgSILENT software. As there were 19 different kinds of wind speed in the wind farm (see appendix Table 1), the wind farm can be represented by 19 sets of parallel fans. Fig.2 shows the detailed model.

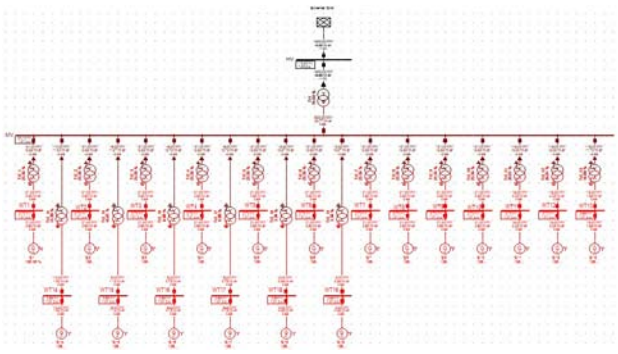

Fig.2. The detailed model of the wind farm

Fig.3 illustrates the output results from simulations using the detailed model of the wind farm in the four scenarios.

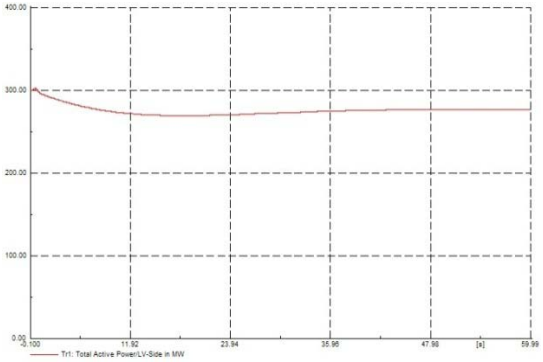

(a) Wind speed of +11.6 m/s, angle = 0°

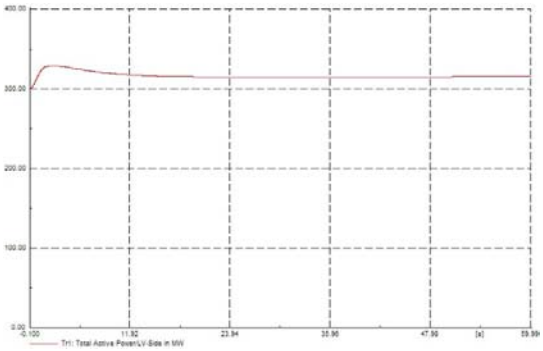

(b) Wind speed of +15 m/s, angle =30°

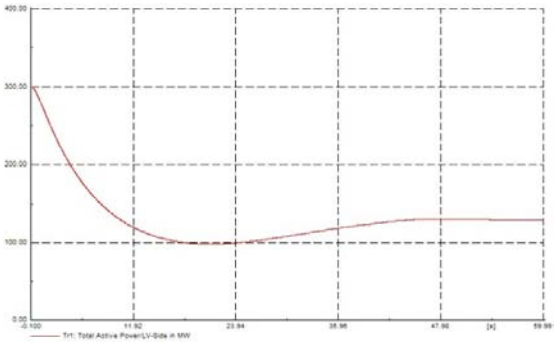

(c) Wind speed of +9 m/s, angle =60°

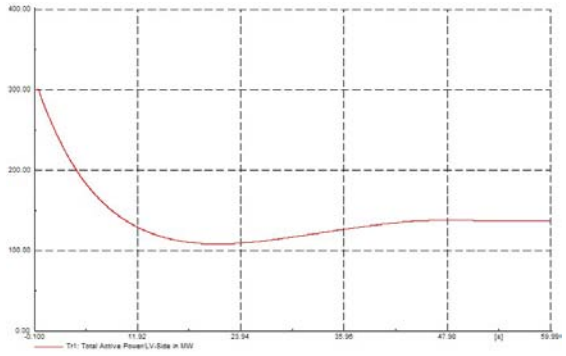

(d) Wind speed of +11.6 m/s, angle =90°

Fig.3. Output of simulations based on the detailed model of wind farm in the four scenarios

As shown in Fig.3(a), at the rated wind speed, the real output of the 300 MW wind farm is 277 MW due to the wake effect. In Fig.3(b), although the wake effect has attenuated the output, the effective input wind speeds of all fans are still higher than the rated wind speed as the input wind speed is much higher than the rated wind speed. Therefore, by controlling the pitch angle, the output of the fans is ultimately slightly higher than the rated output value. In Fig.3(c), as the wind speed is lower than the rated wind speed, the output from the plant is further weakened after attenuation by the wake effect. In Fig.3(d), the intercepted wind energy from the fans is greatly reduced compared with the rated case in Fig.3(a) due to the extreme conditions (i.e. the wind direction is parallel with the row of fans). The actual output from the wind farm is only 137 MW even though the installed capacity is 300 MW. Generally, the front of the row of fans is set towards the dominant wind direction in the region during the establishment of the wind farm, just as in Fig.3(a). Thus, the condition shown in Fig.3(d) is commonly impossible in practice. For some regions in which the variation in the regularity of the wind direction is not obvious, the distance between the fans in the same row can be increased during establishment of the wind farm to reduce the wake effect.

4.2 Aggregation model of the wind farm using the single-fan equivalent method

An aggregation model of the wind farm was built using the single-fan equivalent method. The one hundred DFIGs are taken to be equivalent to one fan with large capacity. Table 1 shows the modifications made to the parameters of the DFIG model before and after aggregation.

Fig.4 lists the output results of wind power at the four scenarios given in Section 4.1 using the single-fan aggregation model.

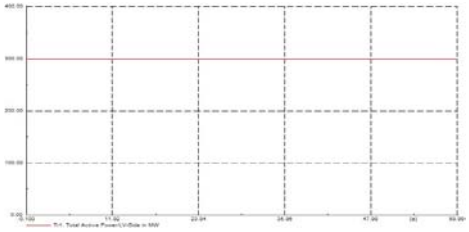

(a) Wind speed of +11.6 m/s, angle = 90°

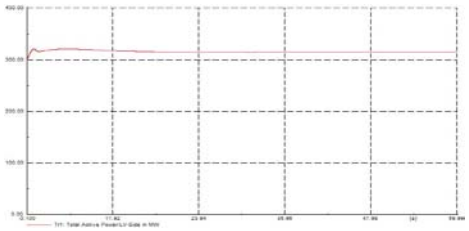

(b) Wind speed of +15 m/s, angle = 30°

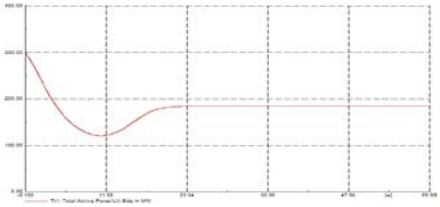

(c) Wind speed of +9 m/s, angle =60°

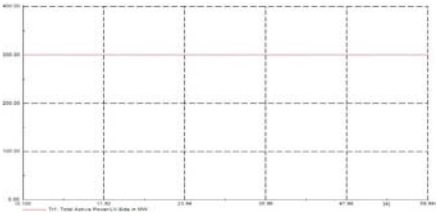

(d) Wind speed of +11.6 m/s, angle = 90°

Fig.4. Output of the simulations based on the single-fan equivalent model in the four scenarios

Fig. 4 suggests that for the different given wind speeds, some differences between the output results from the single-fan equivalent model and detailed model are small while others are larger. When the

wind speed approaches the dominant wind speed in wind farm, the output from wind farm is more accurately reflected by the single-fan equivalent model. Otherwise, the simulation results are seriously inconsistent with the actual situation, as shown in Fig.4(d). In Fig.4(a), at the rated wind speed, the single-fan equivalent model suggests a higher output value than that in the detailed model due to the neglect of attenuation by the wake effect. Comparison of Figs.3(a) and 4(a) implies that, at the rated wind speed, the differences under these conditions are about 7.7% or so. Thus, this figure represents the proportion of the wind energy lost in actual wind farms because of the wake effect.

4.3 Fan aggregation modeling based on multi-fan characterization

The models of four scenarios in Section 4.1 were built using multi-fan characterization. The classification index employed in the K-means clustering algorithm was the equivalent input wind speed of each fan, as shown in appendix Table 1. In the K-means clustering model, we set K_0=4, K_{max}=10, and λ=0.5, i.e. the wind speed was classified into at least four but no more than ten clusters at most. A measurement function smaller than 0.5 was considered to meet accuracy requirement. Thus the calculation can be terminated. Table 2 shows the equivalent parameters of the multi-fan characterization model for the four scenarios.

Using the data in Table 2, the fan clusters were equivalently aggregated. Fig.5 shows the corresponding simulation results in the four scenarios.

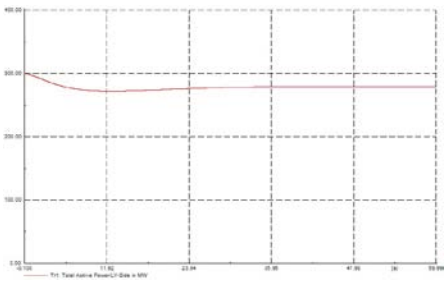

(a) Wind speed of +11.6 m/s, angle = 0°.

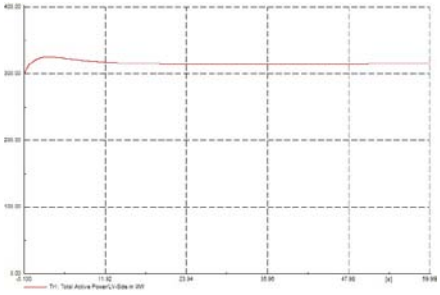

(b) Wind speed of +15 m/s, angle = 30° .

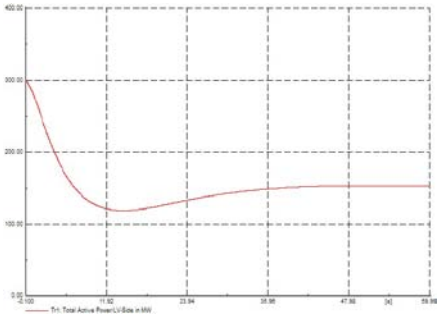

(c) Wind speed of +9 m/s, angle = 60°.

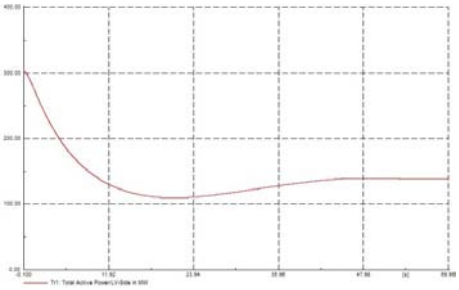

(d) Wind speed of +11.6 m/s, angle = 90°.

Fig.5. Output from the simulations based on the multi-fan characterization in the four scenarios

The multi-fan characterization model is closer to the real condition reflected by the detailed model than the single-fan characterization model shown in Fig.3–Fig.5. Table 3 shows the steady output of the multi-fan aggregation model after simulation for 1 minute. Based on the table 3, the multi-fan aggregation model presents an output phase closer to that of the detailed model than the single-fan equivalent model, especially for the second and third scenario. The error in the second scenario decreased from 32.4% (single-fan aggregation model) to 4.3% (multi-fan aggregation model), while that in the third scenario dropped from 43.9% to 6.0%.

Table 1. Equivalent parameters in the single-fan aggregation model

Index	Single-fan model, before aggregation	Equivalent fan model of the plant after aggregation	Expansion multiple
Rated capacity of the fan set (MVA)	3	300	100
Capacity of the medium voltage step-up transformer (MVA)	3.75	375	100
Capacity of the high voltage step-up transformer (MVA)	4	400	100
Short-circuit capacity of the infinite bus system (MVA)	300	30000	100
Average air density (kg/m^3)	0.0021042	0.443765	210.895
Rotating inertia of the doubly-fed generator (kg·m^2)	6.03	603	100
Shaft elasticity coefficient	120.405	1240.5	100
Output reference value of the fan (MW)	2.25	225	100
Output reference value of the wind motor (MW)	1.970627	197.0627	100
Mutual damping coefficient between the low speed shaft of wind wheel and the high speed shaft of the doubly-fed machine	2.25	225	100
Measurement module reference value of the frequency converter on the rotor side	3	300	100
Rotor overcurrent protection value	2.25	225	100

Table 2. Calculation parameters from the *K*-means clustering model based on multi-fan characterization

Wind speed of +11.6 m/s, angle = 0°	Equivalent fan number	4			
	Equivalent wind speed of each fan (m/s)	10.7158	10.9476	11.1619	11.6
	Aggregated fan number of each fan	18	15	30	37
Wind speed of +15 m/s, angle = 30°	Equivalent fan number	4			
	Equivalent wind speed of each fan (m/s)	14.0386	14.2777	14.5248	14.9159
	Aggregated fan number of each fan	11	14	16	59
Wind speed of +9 m/s, angle = 60°	Equivalent fan number	4			
	Equivalent wind speed of each fan (m/s)	8.0651	8.3013	8.6219	9
	Aggregated fan number of each fan	12	18	34	36
Wind speed of +11.6 m/s,	Equivalent fan number	8			

angle = 90°	Equivalent wind speed of each fan (m/s)	7.9607	8.1608	8.4018	8.6883
	Aggregated fan number of each fan	13	24	21	14
	Equivalent wind speed of each fan (m/s)	8.9611	9.2487	9.7225	11.6
	Aggregated fan number of each fan	7	7	7	7

Table 3. Simulation results of the models after 1 minute of simulation

Simulation condition	Detailed model (MW)	Single-fan equivalent aggregation model (MW)	Error in the single-fan equivalent aggregation model (%)	Multi-fan equivalent aggregation model (MW)	Error in the multi-fan equivalent aggregation model (%)	Detailed model (MW)
Wind speed of +11.6 m/s, angle = 0°	277	300	8.3	280	1.1	277
Wind speed of +15 m/s, angle = 30°	315	316	0.3	315	0	315
Wind speed of +9 m/s, angle = 60°	139	184	32.4	145	4.3	139
Wind speed of +11.6 m/s, angle = 90°	134	300	43.9	142	6.0	134

5 Conclusions

In this paper, a model of 300 MW wind farm in northern Jiangzu Province was built to study the benefits of aggregation modeling for large wind farms considering wake effects. The wind farm was simulated using a detailed model, a single-fan aggregation model, and multi-fan aggregation model respectively. The detailed model accurately reflected the output of the wind farm. However, this model involves a complex modeling process and has a slow simulation speed. The single-fan characterization method is a simple, convenient, and commonly used aggregation method. Unfortunately, it is prone to generate large errors since it ignores the wind energy loss caused by the wake effect. The improved K-means-based multi-fan characterization method put forward in this paper is flexible, accurate, and produces results rapidly when used to build the model of wind farm. The effectiveness and feasibility of the method proposed are verified by taking a 300 MW wind farm in northern Jiangsu Province as computational examples.

References:

[1] Wang Zhen-hao, Liu Jin-long, Li Guoqing, et al, Power and voltage regulation of wind farm based on EDLC energy storage, *Electric Power Automation Equipment*, Vol.31, No.3, 2011, pp. 113-116.

[2] Bai Hong-bin, Wang rui-hong, Influence of the grid connected wind farm on power quality, *Proceedings of the Chinese Society of Universities for Electric Power System and its Automation*, Vol.24, No.1, 2012, pp. 120-124.

[3] Chen Shu-yong, Dai Hui-zhu, Bai Xiao-min, et al, Impact of wind turbine wake on wind power output, *Electric Power*, Vol.31, No.11, 1998, pp. 28-31.

[4] Huang Mei, Wan Hang-yu, Simplification of

wind farm model for dynamic simulation, *Transactions of China Electrotechnical Society*, Vol.24, No.9, 2009, pp. 147-152.

[5] J. Usaola, P. Ledesma, J. M. Rodriguez, et al, Transient stability studies in grid with great wind power generation: Modelling issues and operation requirements, *IEEE Power Engineering Society General Meeting*, Vol.3, 2003, pp. 1534-1541.

[6] L. M. Fernandez, C. A. Garcia, F. Jurado, et al, Aggregation of doubly fed induction generators wind turbines under different incoming wind speeds, *Power Tech IEEE Russia*, 2005, pp. 1-6.

[7] Li Hui, Wang He-sheng, Shi Xu-yang, et al, Study on equivalent model of wind farms based on genetic algorithm, *Power System Protection and Control*, Vol.39, No.11, 2011, pp. 1-8.

[8] Slootweg J G, Kling W L, Modeling of large wind farms in power system simulations, *Proceedings of the IEEE PES Summer Meeting*, 2002, pp. 25-29.

[9] Miguel Garcia-Gracia, Paz Comech M, Jesus Sallan, et al, Modelling wind farms for grid disturbance studies. *Renewable Energy*, Vol.33, No.9, 2008, pp. 2109-2121.

[10] R. M. G., Castro, J. M., Ferreira de Jesus, An aggregated wind park model, *Proceedings of the 13th Power Systems Computation Conference*, 1999, pp. 1-5.

[11] Mi Zeng-qiang, Su Xun-wen, Yang Qi-xun, et al, Multi-machine representation method for dynamic equivalent model of wind farms, *Transactions of China Electrotechnical Society*, Vol.25, No.5, 2010, pp. 162-169.

[12] Yang Shan-lin, Li Yong-sen, Hu Xiao-xuan, et al, Optimization Study on k Value of K-means Algorithm, *Systems Engineering-theory & Practice*, Vol.26, No.2, 2006, pp. 96-101.

[13] Gao Feng, Zhao Dong-lai, Zhou Xiao-xin, et al, Dynamic equivalent algorithm for wind farm composed of direct-drive wind turbines, *Power System Technology*, Vol.36, No.12, 2012, pp. 222-227.

[14] Fu Rong, Xie Jun, Wang Bao-yun, Study on dynamic equivalence model of wind farms with DFIG under wind turbulence, *Power System Protection and Control*, Vol.40, No.15, 2012, pp. 1-6.

[15] Yan Hui-min, Study on plan and policy of wind power development in Jiangsu, *Jiangsu Electrical Engineering*, Vol.24, No.1, 2005, pp. 8-10.

[16] Hájek, P., Neri, F., An introduction to the special issue on computational techniques for trading systems, time series forecasting, stock market modeling, financial assets modeling, *WSEAS Transactions on Business and Economics*, Vol.10, No.4, 2013, pp. 201-292.

[17] Azzouzi, M., Neri, F., An introduction to the special issue on advanced control of energy systems, *WSEAS Transactions on Power Systems*, Vol.8, No.3, 2013, pp. 103.

[18] Bojkovic, Z., Neri, F., An introduction to the special issue on advances on interactive multimedia systems, *WSEAS Transactions on Systems*, Vol.12, No.7, 2013, pp. 337-338.

[19] Pekař, L., Neri, F., An introduction to the special issue on advanced control methods: Theory and application, *WSEAS Transactions on Systems*, Vol.12, No.6, 2013, pp. 301-303.

[20] Guarnaccia, C., Neri, F., An introduction to the special issue on recent methods on physical polluting agents and environment modeling and simulation, *WSEAS Transactions on Systems*, Vol.12, No.2, 2013, pp. 53-54.

[21] Neri, F., An introduction to the special issue on computational techniques for trading systems, time series forecasting, stock market modeling, and financial assets modeling, *WSEAS Transactions on Systems*, Vol.11, No.12, 2012, pp. 659-660.

[22] Muntean, M., Neri, F., Foreword to the special issue on collaborative systems, *WSEAS Transactions on Systems*, Vol.11, No.11, 2012, pp. 617.

[23] Pekař, L., Neri, F. (2012) An introduction to the special issue on time delay systems: Modelling, identification, stability, control and applications, *WSEAS Transactions on Systems*, Vol.11, No.10, 2012, pp. 539-540.

[24] Volos, C., Neri, F., An introduction to the special issue: Recent advances in defense systems: Applications, methodology, technology, *WSEAS Transactions on Systems*, Vol.11, No.9, 2012, pp. 477-478.

[25] ZHANG Jian-ping , Zhang Li-bo CHENG Hao-zhong, et al, Evaluation of Probabilistic Load Flow Based on Improved Latin Hypercube Sampling, *East China Electic Power*, Vol.41, No.10, 2013, pp. 2028-2034.

[26] ZHANG Jian-ping ZHANG Xiang CHENG Hao-zhong, et al, Production Simulation of Power System with Wind Farms Considering EPP Influence, *East China Electic Power*, Vol.41, No.9, 2013, pp. 1804-1807.

[27] ZHANG Jian-ping LIU Jie-feng CHENG Hao-zhong, et al, Saturated Load Forecasting Based on Per Capita Electricity Consumption and Per Capita Electricity Load, *East China Electic Power*, Vol.42, No.4, 2014, pp. 661-664.

Appendix

Appendix Table 1. Equivalent wind speed calculation results for a typical 300MW wind farm in northern Jiangsu Province.

(a) Wind speed of 11.6 m/s, with an angle of 0° in the positive direction

11.60	11.60	11.60	11.60	11.60	11.60	11.60	11.60	11.60	11.60
11.60	11.60	11.60	11.60	11.60	11.60	11.60	11.60	11.60	11.60
11.60	11.60	11.60	11.60	11.60	11.60	11.16	11.16	11.16	11.16
11.16	11.16	11.16	11.16	11.16	11.16	11.16	11.16	11.60	11.60
11.16	11.16	11.16	11.16	11.16	11.16	11.16	11.16	11.16	11.16
11.16	11.16	11.16	11.60	11.60	11.16	10.97	10.97	10.97	10.97
10.97	10.97	10.97	10.97	10.97	10.97	10.97	10.97	11.16	11.60
11.60	11.60	11.16	10.87	10.76	10.76	10.76	10.76	10.76	10.76
10.76	10.76	10.76	10.76	10.76	10.87	11.16	11.60	11.60	11.60
11.60	11.16	10.87	10.64	10.64	10.64	10.64	10.64	10.64	10.64

(b) Wind speed of 15 m/s, with an angle of 30° in the positive direction

15.00	15.00	15.00	15.00	15.00	15.00	15.00	15.00	14.86	15.00
14.86	15.00	15.00	14.86	15.00	15.00	14.86	14.86	15.00	14.86
14.86	15.00	15.00	14.86	14.86	15.00	15.00	14.86	14.86	14.86
14.86	14.86	14.86	15.00	14.86	14.86	14.86	15.00	14.86	14.86
14.52	14.86	14.86	14.86	14.52	14.86	15.00	14.86	14.52	14.86
15.00	14.86	14.52	14.52	14.86	14.86	14.52	14.52	14.86	15.00
14.86	14.52	14.29	14.86	15.00	14.52	14.29	14.52	14.86	14.52
14.29	14.52	14.86	14.52	14.29	14.29	14.86	14.52	14.29	14.23
14.52	14.29	14.04	14.52	14.29	14.04	14.29	14.29	14.04	14.23
14.29	14.04	14.04	14.29	14.04	14.04	14.04	14.04	14.04	14.04

(c) Wind speed of 7 m/s, with an angle of 60° in the positive direction

7.00	7.00	7.00	7.00	7.00	7.00	7.00	7.00	7.00	7.00
7.00	7.00	7.00	7.00	7.00	7.00	7.00	7.00	7.00	7.00
7.00	6.72	7.00	7.00	7.00	7.00	6.72	7.00	6.72	7.00
7.00	6.72	7.00	6.72	7.00	6.72	6.72	7.00	6.72	7.00
6.72	6.72	6.72	6.72	7.00	6.72	6.72	6.72	6.72	6.72
6.72	7.00	6.72	6.72	6.60	6.72	6.72	6.72	7.00	6.60
6.72	6.47	6.72	6.72	6.60	7.00	6.47	6.72	6.47	6.60
6.72	6.47	6.47	6.60	6.47	6.47	6.72	6.47	6.47	6.47
6.47	6.47	6.47	6.39	6.47	6.47	6.39	6.32	6.39	6.32
6.30	6.32	6.30	6.30	6.30	6.30	6.24	6.24	6.19	6.13

(d) Wind speed of 11.6 m/s, with an angle of 90° in the positive direction

11.60	11.60	11.60	9.72	11.60	9.72	11.60	9.72	9.25	11.60

9.72	9.25	11.60	9.72	9.25	8.96	9.72	9.25	8.96	9.72
9.25	8.96	8.76	9.25	8.96	8.76	9.25	8.96	8.76	8.61
8.96	8.76	8.61	8.96	8.76	8.61	8.49	8.76	8.61	8.49
8.76	8.61	8.49	8.40	8.61	8.49	8.40	8.61	8.49	8.40
8.31	8.49	8.40	8.31	8.49	8.40	8.31	8.24	8.40	8.31
8.24	8.40	8.31	8.24	8.31	8.24	8.18	8.31	8.24	8.18
8.24	8.18	8.12	8.24	8.18	8.12	8.18	8.12	8.07	8.18
8.12	8.07	8.12	8.07	8.03	8.12	8.07	8.03	8.07	8.03
7.98	8.03	7.98	7.98	7.95	7.95	7.91	7.91	7.88	7.85